Quantum Anomalous Hall Effect in Magnetically Doped InAs/GaSb Quantum Wells

Qing-Ze Wang,[1] Xin Liu,[1] Hai-Jun Zhang,[2] Nitin Samarth,[1] Shou-Cheng Zhang,[2] and Chao-Xing Liu[1]
[1]*Department of Physics, The Pennsylvania State University, University Park, Pennsylvania 16802-6300, USA*
[2]*Department of Physics, McCullough Building, Stanford University, Stanford, California 94305-4045, USA*
(Received 4 December 2013; published 29 September 2014)

The quantum anomalous Hall effect has recently been observed experimentally in thin films of Cr-doped $(Bi, Sb)_2Te_3$ at a low temperature (~30 mK). In this work, we propose realizing the quantum anomalous Hall effect in more conventional diluted magnetic semiconductors with magnetically doped InAs/GaSb type-II quantum wells. Based on a four-band model, we find an enhancement of the Curie temperature of ferromagnetism due to band edge singularities in the inverted regime of InAs/GaSb quantum wells. Below the Curie temperature, the quantum anomalous Hall effect is confirmed by the direct calculation of Hall conductance. The parameter regime for the quantum anomalous Hall phase is identified based on the eight-band Kane model. The high sample quality and strong exchange coupling make magnetically doped InAs/GaSb quantum wells good candidates for realizing the quantum anomalous Hall insulator at a high temperature.

DOI: 10.1103/PhysRevLett.113.147201 PACS numbers: 85.75.-d, 73.20.-r, 73.43.-f, 75.50.Pp

Introduction.—The quantum anomalous Hall (QAH) state in magnetic topological insulators [1–12] possesses a quantized Hall conductance carried by chiral edge states, similar to the well-known quantum Hall state [13]. However, its physical origin is due to the exchange coupling between electron spin and magnetization, instead of the orbital effect of magnetic fields. Therefore, the QAH effect does not require any external magnetic field or the associated Landau levels [1] and thus has great potential in the application of a new generation of electronic devices with low dissipation.

Nevertheless, it is difficult to search for realistic systems of the QAH effect, mainly due to the stringent material requirements. To realize the QAH effect, the system should be an insulator with a topologically nontrivial band structure. Simultaneously, ferromagnetism is also required in the same system. In realistic materials, it is rare that ferromagnetism coexists with an insulating behavior. For example, the HgTe/CdTe quantum well (QW) is the first quantum spin Hall (QSH) insulator with a topologically nontrivial band structure [14,15]. With magnetization, it was also predicted to be a QAH insulator [4]. However, ferromagnetism cannot be developed spontaneously in this system. Thus, one has to apply an external magnetic field, obstructing the confirmation of the QAH effect. Alternatively, one can consider other two-dimensional (2D) topological insulators with magnetic doping. It was realized that the nontrivial band structure in the Bi_2Te_3 family of materials can significantly enhance spin susceptibility and may lead to ferromagnetism in the insulating state [6]. Consequently, these systems with magnetic doping become a suitable platform to observe the QAH effect. The recent experimental discovery [9] confirmed this prediction by transport measurements on thin films of Cr-doped $(Bi, Sb)_2Te_3$. In this experiment, the quantized Hall conductance was observed at a low temperature, around ~30 mK, presumably due to the small band gap opened by exchange coupling and low carrier mobility ~760 $cm^2/V\,s$. Therefore, searching for realistic systems with nontrivial band structures, strong exchange coupling, and high sample quality is essential to realizing the QAH effect at a higher temperature. The QAH effect has also been theoretically predicted in other types of systems [5,7,8,12,16–18].

Here, we propose a new system for the QAH effect, magnetically doped InAs/GaSb type-II QWs. The InAs/GaSb QW is predicted to be a QSH insulator with a certain range of well thickness [19]. Transport experiments have indeed observed a stable longitudinal conductance plateau with a value of $2e^2/h$ in this system [20–23]. Moreover, Mn-doped InAs and GaSb are known diluted magnetic semiconductors [24–26]. High quality heterostructures integrating (In,Mn)As and GaSb have been fabricated by molecular beam epitaxy [27]. Unlike the case of Mn-doped GaAs where debate continues about the origin of ferromagnetic ordering [28–30], the ferromagnetism in Mn-doped InAs is consistent with free-hole-mediated ferromagnetism within a mean field Zener model [31–34]. Magnetically doped InAs/GaSb heterostructures are also attractive for optical control [35] and electric field control [36] of carrier-mediated ferromagnetism. Therefore, it is natural to ask whether the QAH effect can be realized in this system. In this work, we find the Curie temperature of ferromagnetism can be significantly enhanced due to the nontrivial band structure. The quantized Hall conductance appears in a wide regime of parameters below the Curie temperature. Therefore, magnetically doped InAs/GaSb QWs provide a promising platform to search for the QAH effect with a high critical temperature.

InAs/GaSb quantum wells and ferromagnetism.—A schematic plot is presented in Fig. 1(a) for InAs/GaSb QWs, in which InAs and GaSb together serve as well layers and AlSb layers are for barriers [37–39]. The unique feature of InAs/GaSb QWs is that the conduction band minimum of InAs has lower energy than the valence band maximum of GaSb, due to the large band offset. Consequently, when the well thickness is large enough, the first electron subband of InAs layers, denoted as $|E_1\rangle$, lies below the first hole subband of GaSb layers, denoted as $|H_1\rangle$. This special band alignment is similar to that in HgTe QWs, known as an "inverted band structure," which is essential for the QSH effect [19,21]. Since the $|H_1\rangle$ state has a higher energy than the $|E_1\rangle$ state, there is an intrinsic charge transfer between InAs and GaSb layers. This can be seen from the energy dispersion in Fig. 1(b), where the Fermi energy (dashed line) crosses both the $|E_1\rangle$ band in the InAs layer (solid blue line) and the $|H_1\rangle$ band in the GaSb layer (solid red line) if we neglect the coupling between two layers. Clearly, the InAs layer is electron doped while the GaSb layer is hole doped. With magnetic doping, free carriers in the InAs and GaSb layers are able to mediate exchange coupling between magnetic moments through a Ruderman-Kittel-Kasuya-Yosida interaction [31,33,40,41], leading to ferromagnetism in these systems with the Curie temperature $T_c \sim 25$ K [26]. Therefore, we expect that magnetically doped InAs/GaSb QWs in the metallic phase of Fig. 1(b) should also be ferromagnetic. The problem is complicated by the coupling between two layers, which induces a hybridization gap, as shown in Fig. 1(c) or Fig. 1(d). Therefore, it is natural to ask what happens to ferromagnetism for the insulating regime with the Fermi energy in the hybridization gap. Below, we will answer this question by studying a four-band model.

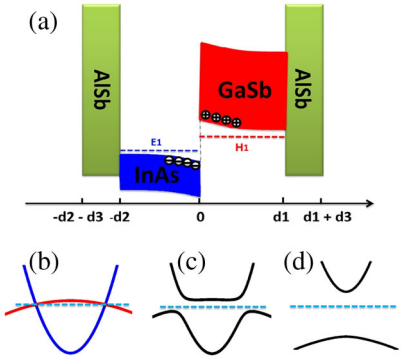

FIG. 1 (color online). (a) Illustration of an AlSb/InAs/GaSb/AlSb type-II semiconductor QW. The widths of AlSb, InAs, and GaSb are denoted as d_3, d_2, and d_1, respectively. In the inverted regime, hole subbands of GaSb are located above electron subbands of InAs, leading to an electric charge transfer between these two layers. (b)–(d) Band structures for InAs/GaSb QWs with $A = 0$ eV · Å, $A = 0.3$ eV · Å, and $A = 2$ eV · Å, respectively; A is the coupling strength between the first hole subband of GaSb and the first electron subband of InAs.

The low energy physics of magnetically doped InAs/GaSb QWs can be well described by a four-band model, which was first developed by Bernevig-Hughes-Zhang for HgTe QWs [14,19]. In the basis of $|E_1+\rangle$, $|H_1+\rangle$, $|E_1-\rangle$, and $|H_1-\rangle$, the effective Hamiltonian can be expressed as

$$H = H_0 + H_{\mathrm{BIA}} + H_{\mathrm{SIA}} + H_{\mathrm{ex}}. \tag{1}$$

The Bernevig-Hughes-Zhang Hamiltonian H_0 is given by

$$H_0 = \epsilon_k \mathbf{1}_{4\times4} + \mathcal{M}(\vec{k})\sigma_0 \otimes \tau_z + Ak_x\sigma_z \otimes \tau_x - Ak_y\sigma_0 \otimes \tau_y,$$

where $\epsilon_k = C - D(k_x^2 + k_y^2)$, $\mathcal{M}(\vec{k}) = M_0 - B(k_x^2 + k_y^2)$, $\mathbf{1}_{4\times4}$ is a 4×4 identity matrix, and σ and τ are Pauli matrices, representing spin and subbands, respectively. All the parameters used below are given in the Supplemental Material [42] for InAs/GaSb QWs. The linear term (A term) couples electron subbands of InAs and hole subbands of GaSb and opens a hybridization gap. H_{BIA} and H_{SIA} describe bulk inversion asymmetry and structural inversion asymmetry [19,42]. H_{ex} describes the exchange coupling between magnetic moments and electron spin. In the basis of the four-band model, we can write H_{ex} as

$$H_{\mathrm{ex}} = \sum_{\vec{R}_n} \mathbf{S}_M(\vec{R}_n) \cdot \tilde{\mathbf{s}}, \tag{2}$$

where $\mathbf{S}_M(\vec{R}_n)$ denotes the magnetic impurity spin at the position $\vec{R}_n$ and $\tilde{\mathbf{s}}$ is regarded as an effective spin operator of the four-band model. We should emphasize that both the total angular momentum and exchange coupling constants are included in $\tilde{\mathbf{s}}$ for simplicity. (See the Supplemental Material for details [42].) We only consider magnetization along the z direction, and the operator $\tilde{s}_z$ can be decomposed into

$$\tilde{s}_z = s_1\sigma_z \otimes \tau_z + s_2\sigma_z \otimes \tau_0, \tag{3}$$

where $(s_1 + s_2)\sigma_z$ $[(-s_1 + s_2)\sigma_z]$ describes the effective spin operator for the conduction [valence] band in the four-band model.

Next, we determine the Curie temperature of ferromagnetism in this system through the standard mean field theory. With linear response theory, the spin susceptibility for the operator $\tilde{s}_z$ is given by

$$\tilde{\chi}_s = \lim_{q\to0} \mathrm{Re}\left[\sum_{i,j,\sigma,\sigma',\vec{k}} \frac{|\langle u_{i\sigma,\vec{k}}|\tilde{s}|u_{j\sigma',\vec{k}+\vec{q}}\rangle|^2 [f_{i\sigma}(\vec{k}) - f_{j\sigma'}(\vec{k}+\vec{q})]}{E_{j\sigma'}(\vec{k}+\vec{q}) - E_{i\sigma}(\vec{k}) + i\Gamma}\right], \tag{4}$$

where i and j denote conduction and valence bands, σ and σ' are spin indices, $u_{i\sigma}$ is the eigenwave function with the energy $E_{i\sigma}$, $f_{i\sigma}(\vec{k})$ is the Fermi-Dirac distribution function, and Γ is band broadening, estimated as $\sim10^{-4}$ eV [20]. The susceptibility of the magnetic moment takes the form $\tilde{\chi}_M = S_0(S_0 + 1)/3k_BT$, which is obtained from the dilute limit of Curie-Weiss behavior. S_0 is the spin magnitude of

magnetic impurities. The Curie temperature can be determined by the condition $N_0 x_{\text{eff}} \tilde{\chi}_s(T_c)\tilde{\chi}_M(T_c) = 1$ [40,42] in the mean field approximation, where N_0 is the cation concentration and x_{eff} is the effective composition of magnetic atoms.

As described above, in the absence of the coupling between two layers, the system must be in a ferromagnetic phase. This corresponds to the case with $A = 0$ in the four-band model. Therefore, we treat A as a parameter and plot the calculated Curie temperature T_c as a function of A and Fermi energy E_f, as shown in Fig. 2(a). When the Fermi energy lies in the hybridization gap (around 0 meV), the Curie temperature first increases and then decreases with the increasing of A. Therefore, we find surprisingly that the opening of a small hybridization gap will enhance ferromagnetism.

To understand the underlying physics, we consider different origins of spin susceptibility. According to Eq. (4), spin susceptibility can be separated into two parts: the intraband contribution ($i = j$) and the interband contribution ($i \neq j$). The intraband contribution originates from the states near Fermi energy and mediates the Ruderman-Kittel-Kasuya-Yosida type of coupling between magnetic moments. It is the main origin for ferromagnetism in metallic systems. Indeed, our calculation shows that the intraband contribution has a maximum around the band edge because of the singularity of the density of states [Fig. 2(d)] [51,52] but is significantly reduced when the Fermi energy is tuned into the band gap [the solid blue line in Fig. 2(c)]. On the other hand, the interband contribution mainly originates from the hybridization of wave functions between conduction and valence bands due to the inverted band structure, known as the Van Vleck mechanism, according to Ref. [6]. Therefore, the interband contribution shows a peak in the insulating regime and diminishes as the Fermi energy goes away from the band gap. Taking into account both contributions, we find sharp peaks of the total spin susceptibility near band edges at low temperatures (below 4 K), as shown in Fig. 2(b). With increasing temperatures, both peaks are smeared and the spin susceptibility reveals a broad peak structure around the band gap, leading to the enhancement of the Curie temperature T_c in the insulating regime.

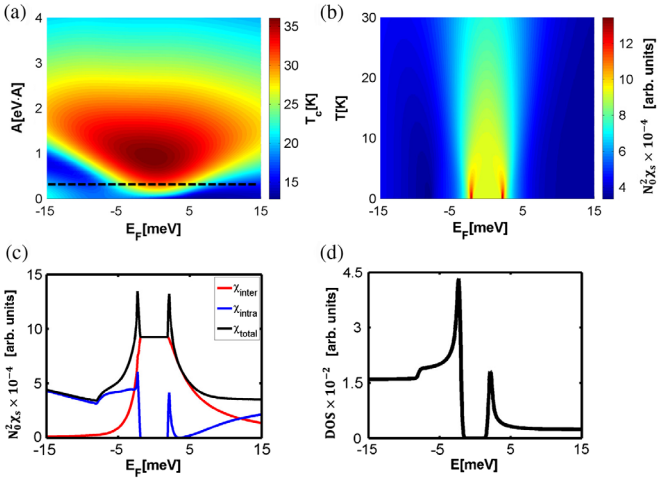

FIG. 2 (color online). (a) Curie temperatures as a function of the parameter A and Fermi energy. The dashed black line denotes the case with $A = 0.3$ eV · Å. (b) Total spin susceptibility χ_s as a function of Fermi energy E_f and temperature. (c) Different contributions (intraband and interband contributions) to spin susceptibility χ_s at $T = 0$ K, respectively. (d) Density of states (DOS) for an InAs/GaSb quantum well with a hybridization gap.

It is necessary to compare the magnetic mechanism in magnetically doped InAs/GaSb QWs with that in Mn-doped HgTe QWs and Cr-doped $(\text{Bi, Sb})_2\text{Te}_3$. The low energy effective Hamiltonian of HgTe QWs takes the same form as the Hamiltonian in Eq. (2). However, there is one essential difference: the parameter A is much larger in HgTe QWs because electron and hole subbands are in the same layer and coupled strongly. For a large A, spin susceptibility will be suppressed due to the large band gap and the disappearance of band edge singularity, as shown in Fig. 1(d). Consequently, ferromagnetism is not favorable in Mn-doped HgTe QWs [4]. The strong interband contribution in our case is similar to that in Cr-doped $(\text{Bi, Sb})_2\text{Te}_3$. The s_1 term of the effective spin operator [Eq. (3)] takes the same form as that in the effective model of Cr-doped $(\text{Bi, Sb})_2\text{Te}_3$ (see Ref. [6]), which mainly contributes to the interband spin susceptibility. Equation (3) includes an additional part $s_2\sigma_z \otimes \tau_0$, which dominates the intraband contribution. Our calculation shows that both parts of the spin operator have a significant contribution to spin susceptibility in the case of a small hybridization gap and a band edge singularity. Therefore, in the regime favorable for QAH, a relatively high Curie temperature for ferromagnetism ($T_C \sim 30$ K) is expected for magnetically doped InAs/GaSb QWs in comparison with the Cr-doped Bi chalcogenides.

Quantized Hall transport and realistic systems.—Our calculations clearly show that ferromagnetism can be developed in magnetically doped InAs/GaSb QWs. Below T_c, magnetic moments align and induce a Zeeman-type spin splitting for both conduction and valence bands due to exchange coupling. To realize the QAH states, spin splitting needs to exceed the band gap. This situation is similar to that of Mn-doped HgTe QWs. From Ref. [4], we find that two conditions for the QAH effect should be satisfied: (1) one spin block becomes a normal band ordering while the other spin block remains in an inverted band ordering, and (2) the system stays in an insulating state [42]. The first condition is satisfied in InAs/GaSb QWs by controlling magnetic doping [37–39], while the second condition can be achieved by tuning well thickness. Once these two conditions are satisfied, the QAH effect is expected.

At a low temperature, the average spin $\langle S_M \rangle$ of magnetic atoms and the average effective spin polarization $\langle \tilde{s}_z \rangle$ can be numerically calculated self-consistently [42,53]. The magnetization of magnetic dopants as a function of the Fermi level and temperature is shown in Fig. 3(a). The critical

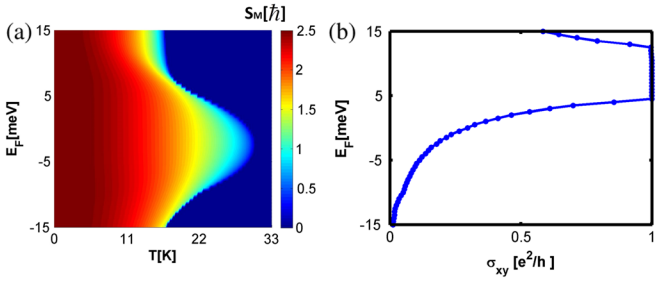

FIG. 3 (color online). (a) Magnetization of Mn as a function of temperature and the Fermi energy. (b) The Hall conductance as a function of Fermi energy E_F at the temperature $T = 1$ K.

temperature for ferromagnetic order determined in Fig. 3(a) is consistent with the early calculation based on spin susceptibility. With the obtained magnetization, we compute the Hall conductivity at $T = 1$ K with the standard Kubo formula [54,55]. As seen in Fig. 3(b), the Hall conductance is quantized at a value of e^2/h when the Fermi energy falls in the band gap and decreases in the metallic regime.

Two key ingredients in the above analysis are the small hybridization gap and the band edge singularity, which have been observed in transport experiments of InAs/GaSb QWs [21,23,56]. Therefore, although our calculation is based on a simple four-band model, all the arguments should remain valid qualitatively in realistic materials. Quantitatively, to determine the regime of the QAH effect, we perform an electronic band structure calculation with an eight-band Kane model [57,58]. The validity of the Kane model has been justified by comparing with the *ab initio* calculations, as shown in the Supplemental Material [42]. The band gap as a function of d_{InAs} and spin of a magnetic atom S_M is plotted in Fig. 4, from which we can extract the phase diagram. With increasing magnetization, we find a gap closing line in the phase diagram, at which the energy dispersion reveals a single Dirac cone type of band

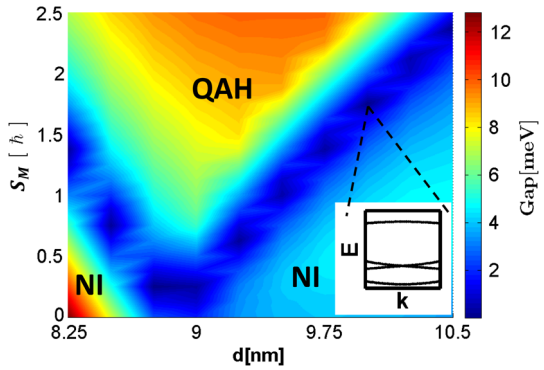

FIG. 4 (color online). The band gap is shown as a function of the well thickness of the InAs layer and the spin of magnetic impurities. The blue color in the figure shows a gap closing line separating the QAH phase from the normal insulator (NI) phase. The inset image shows a Dirac dispersion at the transition point. All the parameters for the Kane model in the calculation are shown in the Supplemental Material [42].

crossing, as shown in the inset of Fig. 4. The Hall conductance will change by $\pm e^2/h$ across a Dirac cone type of transition. Therefore, the system is in the QAH phase for large magnetization. With an experimentally achievable magnetic doping concentration [42], our calculation gives a band gap as high as 10 meV for the QAH phase. The exchange coupling induced band gap is large enough to host the QAH effect at a high temperature.

Discussion and conclusion.—In conclusion, we have proposed a promising material system for the observation of QAH states at relatively high temperatures ($T \sim 30$ K). The materials involved—Mn-doped InAs/GaSb QWs—are already well known to show carrier-mediated ferromagnetism [25,26,34,59]. In the absence of Mn doping and at zero bias, InAs/GaSb QWs have electron-type carriers with a concentration of $\sim 7 \times 10^{11}$ cm^{-2} [20]. Since Mn doping adds holes, we estimate a doping of 0.014% Mn atoms to compensate electron carriers and to shift the chemical potential to the hybridization gap. Additional Mn doping will introduce p-type carriers, which can be diminished by tuning the front and back gates. To further increase Mn doping, a compensation doping might be required. Another advantage of InAs/GaSb QWs is the high sample quality with potentially a large mobility of 6000 cm^2/V s for p-type carriers in nonmagnetic heterostructures [23], although it is expected to be somewhat smaller in Mn-doped samples [60]. Because of the strong exchange coupling, the band gap of the QAH state is able to reach 10 meV, far above the Curie temperature of ferromagnetism (around 30 K). Thus, a well-defined quantized Hall conductance plateau will be expected when the temperature is the energy gap induced by exchange coupling. The corresponding experiment is feasible in the present experimental condition. Our calculation based on the standard Zener model has shown a high critical temperature for the QAH effect in magnetically doped InAs/GaSb QWs, which will provide a basis for new spintronics devices with low dissipation.

We would like to thank Kai Chang, Rui-rui Du, Fu-chun Zhang, Jianhua Zhao, and Yi Zhou for useful discussions. This work is supported by the Defense Advanced Research Projects Agency Microsystems Technology Office, MesoDynamic Architecture Program (MESO), through Contracts No. N66001-11-1-4105 and No. N66001-11-1-4110, and in part by FAME, one of six centers of STARnet, a Semiconductor Research Corporation program sponsored by MARCO and DARPA. S. C. Z acknowledges the support by the Department of Energy, Office of Basic Energy Sciences, Division of Materials Sciences and Engineering, under Contract No. DE-AC02-76SF00515.

[1] F. D. M. Haldane, Phys. Rev. Lett. **61**, 2015 (1988).
[2] X.-L. Qi, Y.-S. Wu, and S.-C. Zhang, Phys. Rev. B **74**, 085308 (2006).

[3] X.-L. Qi, T. L. Hughes, and S.-C. Zhang, Phys. Rev. B **78**, 195424 (2008).
[4] C.-X. Liu, X.-L. Qi, X. Dai, Z. Fang, and S.-C. Zhang, Phys. Rev. Lett. **101**, 146802 (2008).
[5] C. Wu, Phys. Rev. Lett. **101**, 186807 (2008).
[6] R. Yu, W. Zhang, H.-J. Zhang, S.-C. Zhang, X. Dai, and Z. Fang, Science **329**, 61 (2010).
[7] J. Ding, Z. Qiao, W. Feng, Y. Yao, and Q. Niu, Phys. Rev. B **84**, 195444 (2011).
[8] H. Zhang, C. Lazo, S. Blügel, S. Heinze, and Y. Mokrousov, Phys. Rev. Lett. **108**, 056802 (2012).
[9] C.-Z. Chang *et al.*, Science **340**, 167 (2013).
[10] Z. F. Wang, Z. Liu, and F. Liu, Phys. Rev. Lett. **110**, 196801 (2013).
[11] J. Wang, B. Lian, H. Zhang, Y. Xu, and S.-C. Zhang, Phys. Rev. Lett. **111**, 136801 (2013).
[12] X.-L. Zhang, L.-F. Liu, and W.-M. Liu, Sci. Rep. **3**, 2908 (2013).
[13] K. v. Klitzing, G. Dorda, and M. Pepper, Phys. Rev. Lett. **45**, 494 (1980).
[14] B. A. Bernevig, T. L. Hughes, and S.-C. Zhang, Science **314**, 1757 (2006).
[15] M. König, S. Wiedmann, C. Brne, A. Roth, H. Buhmann, L. W. Molenkamp, X.-L. Qi, and S.-C. Zhang, Science **318**, 766 (2007).
[16] X. Liu, H.-C. Hsu, and C.-X. Liu, Phys. Rev. Lett. **111**, 086802 (2013).
[17] H.-C. Hsu, X. Liu, and C.-X. Liu, Phys. Rev. B **88**, 085315 (2013).
[18] H. Zhang, J. Wang, G. Xu, Y. Xu, and S.-C. Zhang, Phys. Rev. Lett. **112**, 096804 (2014).
[19] C. Liu, T. L. Hughes, X.-L. Qi, K. Wang, and S.-C. Zhang, Phys. Rev. Lett. **100**, 236601 (2008).
[20] I. Knez, R. R. Du, and G. Sullivan, Phys. Rev. B **81**, 201301 (2010).
[21] I. Knez, R.-R. Du, and G. Sullivan, Phys. Rev. Lett. **107**, 136603 (2011).
[22] K. Suzuki, Y. Harada, K. Onomitsu, and K. Muraki, Phys. Rev. B **87**, 235311 (2013).
[23] L. Du, I. Knez, G. Sullivan, and R.-R. Du, arXiv:1306.1925.
[24] S. Von Molnar, H. Munekata, H. Ohno, and L. Chang, J. Magn. Magn. Mater. **93**, 356 (1991).
[25] H. Ohno, H. Munekata, T. Penney, S. von Molnár, and L. L. Chang, Phys. Rev. Lett. **68**, 2664 (1992).
[26] Y. Nishitani, M. Endo, F. Matsukura, and H. Ohno, Physica (Amsterdam) **42E**, 2681 (2010).
[27] H. Munekata, A. Zaslavsky, P. Fumagalli, and R. Gambino, Appl. Phys. Lett. **63**, 2929 (1993).
[28] N. Samarth, Nat. Mater. **11**, 360 (2012).
[29] B. Chapler, S. Mack, L. Ju, T. Elson, B. Boudouris, E. Namdas, J. Yuen, A. Heeger, N. Samarth, M. Di Ventra *et al.*, Phys. Rev. B **86**, 165302 (2012).
[30] J. Fujii *et al.*, Phys. Rev. Lett. **111**, 097201 (2013).
[31] T. Dietl, H. Ohno, F. Matsukura, J. Cibert, and D. Ferrand, Science **287**, 1019 (2000).
[32] A. MacDonald, P. Schiffer, and N. Samarth, Nat. Mater. **4**, 195 (2005).
[33] T. Jungwirth, J. Sinova, J. Mašek, J. Kučera, and A. H. MacDonald, Rev. Mod. Phys. **78**, 809 (2006).
[34] T. Dietl, Nat. Mater. **9**, 965 (2010).
[35] S. Koshihara, A. Oiwa, M. Hirasawa, S. Katsumoto, Y. Iye, C. Urano, H. Takagi, and H. Munekata, Phys. Rev. Lett. **78**, 4617 (1997).
[36] H. Ohno, D. Chiba, F. Matsukura, T. Omiya, E. Abe, T. Dietl, Y. Ohno, and K. Ohtani, Nature (London) **408**, 944 (2000).
[37] L. Chang and L. Esaki, Surf. Sci. **98**, 70 (1980).
[38] M. J. Yang, C. H. Yang, B. R. Bennett, and B. V. Shanabrook, Phys. Rev. Lett. **78**, 4613 (1997).
[39] E. Halvorsen, Y. Galperin, and K. A. Chao, Phys. Rev. B **61**, 16743 (2000).
[40] T. Dietl, H. Ohno, and F. Matsukura, Phys. Rev. B **63**, 195205 (2001).
[41] K. Sato, L. Bergqvist, J. Kudrnovský, P. H. Dederichs, O. Eriksson, I. Turek, B. Sanyal, G. Bouzerar, H. Katayama-Yoshida, V. A. Dinh, T. Fukushima, H. Kizaki, and R. Zeller, Rev. Mod. Phys. **82**, 1633 (2010).
[42] See Supplemental Material at http://link.aps.org/supplemental/10.1103/PhysRevLett.113.147201, which includes Refs. [6,26,39–41,43–50], for our derivation of the four-band Hamiltonian, a self-consistent calculation of ferromagnetism, and the first-principles calculations.
[43] K. Burch, D. Awschalom, and D. Basov, J. Magn. Magn. Mater. **320**, 3207 (2008).
[44] R. Winkler, *Spin-Orbit Coupling Effects in Two-Dimensional Electron and Hole Systems* (Springer, New York, 2003).
[45] N. W. Ashcroft and N. D. Mermin, *Solid State Physics* (Cengage Learning, New York, 1976).
[46] M. Abolfath, T. Jungwirth, J. Brum, and A. H. MacDonald, Phys. Rev. B **63**, 054418 (2001).
[47] X. Liu, W. Lim, L. Titova, T. Wojtowicz, M. Kutrowski, K. Yee, M. Dobrowolska, J. Furdyna, S. Potashnik, M. Stone *et al.*, Physica (Amsterdam) **20E**, 370 (2004).
[48] J. P. Perdew, K. Burke, and M. Ernzerhof, Phys. Rev. Lett. **77**, 3865 (1996).
[49] G. Kresse and D. Joubert, Phys. Rev. B **59**, 1758 (1999).
[50] G. D. Sanders, Y. Sun, F. V. Kyrychenko, C. J. Stanton, G. A. Khodaparast, M. A. Zudov, J. Kono, Y. H. Matsuda, N. Miura, and H. Munekata, Phys. Rev. B **68**, 165205 (2003).
[51] J. Wang, H. Mabuchi, and X.-L. Qi, Phys. Rev. B **88**, 195127 (2013).
[52] D.-H. Xu, J.-H. Gao, C.-X. Liu, J.-H. Sun, F.-C. Zhang, and Y. Zhou, Phys. Rev. B **89**, 195104 (2014).
[53] T. Jungwirth, W. A. Atkinson, B. H. Lee, and A. H. MacDonald, Phys. Rev. B **59**, 9818 (1999).
[54] D. J. Thouless, M. Kohmoto, M. P. Nightingale, and M. den Nijs, Phys. Rev. Lett. **49**, 405 (1982).
[55] N. A. Sinitsyn, J. E. Hill, H. Min, J. Sinova, and A. H. MacDonald, Phys. Rev. Lett. **97**, 106804 (2006).
[56] I. Knez and R.-R. Du, Front. Phys. **7**, 200 (2012).
[57] J. Li, W. Yang, and K. Chang, Phys. Rev. B **80**, 035303 (2009).
[58] A. Zakharova, S. T. Yen, and K. A. Chao, Phys. Rev. B **64**, 235332 (2001).
[59] E. Abe, F. Matsukura, H. Yasuda, Y. Ohno, and H. Ohno, Physica (Amsterdam) **7E**, 981 (2000).
[60] Y. Matsuda, G. Khodaparast, M. Zudov, J. Kono, Y. Sun, F. Kyrychenko, G. Sanders, C. Stanton, N. Miura, S. Ikeda *et al.*, Phys. Rev. B **70**, 195211 (2004).